Research Article

Journal of Molecular Recognition

Received: 14 August 2009, Revised: 30 September 2009, Accepted: 8 October 2009, Published online in Wiley InterScience: 25 November 2009

(www.interscience.wiley.com) DOI:10.1002/jmr.1003

Thermodynamic and structural analysis of interactions between peptide ligands and SEB

Fahriye Ceyda Dudak[a], Esra Acar Soykut[a], Murat Erman Oğuz[b], Fatih Yaşar[b] and İsmail Hakkı Boyacı[a]*

Staphylococcal enterotoxin B (SEB) is an exotoxin produced by *Staphylococcus aureus* and commonly associated with food poisoning. In this study, SEB-binding peptides were identified by screening a phage displayed peptide library. The binding of peptides to SEB was tested with isothermal titration calorimetry (ITC) and of the five selected peptides, three showed affinity to SEB, with one measured to have the highest affinity constant ($10^5\ M^{-1}$). ITC revealed that the interaction of peptide ligands with SEB was driven entropically and the binding was dominated by hydrophobic interactions. Circular dichroism (CD) measurements and molecular dynamics (MD) simulations, together, give a structural insight into the interaction of peptides with SEB. While SEB binding peptides showed random coil structure before binding, after complex formation they had more ordered structures. The peptide with highest affinity to SEB showed stable conformation during MD simulation. Taken together, our approach about thermodynamic and structural characterization of peptide ligands can be used to develop aptamers, with high affinity and selectivity, for biosensor applications. Copyright © 2009 John Wiley & Sons, Ltd.

Keywords: staphylococcal enterotoxin B (SEB); phage display; peptide ligands; isothermal titration calorimetry (ITC); circular dichroism (CD); molecular dynamics (MD)

INTRODUCTION

Phage display technology is a combinatorial biology approach, based on the fusion of polypeptides on bacteriophage coat proteins and has proven to be a powerful tool for protein–ligand interaction studies (Smith, 1985; Smith and Petrenko, 1997). Phage display provides the selection and identification of peptides binding to a variety of proteins by screening of extremely large and diverse libraries of DNA-encoded peptides (Sidhu *et al*., 2003). Although phage display techniques have been used for numerous biological studies such as designing high affinity super antigens (Enever *et al*., 2005), mapping functional binding sites (Sidhu *et al*., 2003), and identification of peptide binders to inorganic materials (Sarikaya *et al*., 2003), the greatest interest has been aroused for development of peptide ligands as recognition reagents for a specific protein target.

In conventional approach, ligand molecules, namely antibodies, for target molecules are produced mostly in a host organism. Although there have been some important improvements for the production of antibodies, such as hibridoma technologies, there are still some drawbacks such as time and labor-intensive production and low stability. These disadvantages of antibodies have given rise to the selection of peptide ligands, having various advantages over antibodies (Petrenko and Vodyanoy, 2003; Ladner *et al*., 2004). Phage displayed peptides have been selected against various analytes like botulinum neurotoxins (Zdanovsky *et al*., 2001), toxic shock syndrome toxin-1 (Mourez *et al*., 2001), *Bacillus* spores (Turnbough, 2003), and microcystin-LR (Zhao *et al*., 2005). Several researchers reported the potential of peptide ligands as probes in biosensors (Samoylov *et al*., 2002; Petrenko and Sorokulova, 2004).

New ligand molecules were investigated for the detection of toxins, especially the ones which are the cause of widespread intoxications. Staphylococcal enterotoxin B (SEB), produced by *Staphylococcus aureus*, is a significant cause of food poisoning in humans and it is considered to have a potential to be used as biological weapon due to its high stability against heat and proteolytic enzymes (Ler *et al*., 2006). Biosensors, in which antibodies used as recognition agents, based on piezoelectric crystal sensors (Harteveld *et al*., 1997; Lin and Tsai, 2003), surface plasmon resonance (SPR) sensors (Homola *et al*., 2002; Naimushin *et al*., 2002, Slavik *et al*., 2002), and fiber optic sensors (King *et al*., 1999) have been developed for rapid and sensitive detection of SEB.

Although previous applications have been successfully applied by utilizing SEB antibodies as recognition elements, research was directed for creating new aptamers to replace antibodies. In this context, Goldman *et al*. (2000) demonstrated that 12-mer phage displayed peptide binding to SEB with high selectivity, which can be used in biosensor applications, and compared the affinities of selected phage body as a whole and anti-SEB antibody in a fluorometric immunoassay. Similarly another SEB binding

* *Correspondence to: Dr İ. H. Boyacı, Department of Food Engineering, Hacettepe University, Beytepe TR 06800, Ankara, Turkey.*
E-mail: ihb@hacettepe.edu.tr

a *F. C. Dudak, E. A. Soykut, İ. H. Boyacı*
Department of Food Engineering, Hacettepe University, Beytepe 06800, Ankara, Turkey

b *M. E. Oğuz, F. Yaşar*
Department of Physic Engineering, Hacettepe University, Beytepe 06800, Ankara, Turkey

peptide was screened and selected by Wang *et al*. (2004) using a solid phase combinatorial library. The binding specificity and affinity of this peptide was investigated by an HPLC flow analysis and affinity purification of SEB molecule was successfully realized in a column that SEB binding peptides used as affinity agents. In our previous study, the thermodynamic constants of the interaction between SEB and peptide ligand, isolated from a 12-mer phage displayed library, were determined and the binding constant of peptide was compared with that of antibody for the first time in the literature (Soykut *et al*., 2008). Comparison of the affinity of the phage display selected peptides with the commercially available antibodies is important to test the effectiveness and usability of the novel peptide ligands. These previous studies about developing a peptide ligand for SEB suggested improving the affinities of the selected peptides by rational approaches in order to use peptides in biosensors instead of antibodies. Although there are studies for characterization of the peptides in the literature, there is a need for a better understanding for the mechanism of the protein–ligand interactions for a successful redesign of the available ligand peptides.

Molecular dynamic (MD) simulation is one of the most popular computational tools that has been widely applied to biological macromolecules such as proteins and peptides to gain insight into their dynamics, for studying folding/unfolding, and to investigate secondary structures (Seibert *et al*., 2005; Goud *et al*., 2008; Schaeffer *et al*., 2008). MD simulations consider small size systems of a few nanometers and compute the interactions between the components of a molecular system as a function of time. Nowadays, MD simulations are used by laboratory experimentalist not only to interpret experimental results but also to find appropriate experimental conditions, and to test methods in order to study a particular phenomenon (Klepeis *et al*., 2009).

In this study, SEB binding peptides were selected from a phage display library. The thermodynamic aspects of peptide–SEB interaction were studied by isothermal titration calorimetry (ITC). By circular dichroism (CD) spectroscopy, the secondary structures of selected peptides were characterized. The selected peptides were also studied via MD method to gain insight into their conformational structures. We presented a pioneering approach to reveal the mechanism of the protein–ligand interaction from the point of structure–activity relationship for phage display selected SEB binding peptides. The results provide us a better understanding for the available SEB binding peptides, which will help one to redesign available peptide ligands with superior affinities.

MATERIALS AND METHODS

Reagents

M13 phage display (PhD) library and the host organism, *Escherichia coli* ER2738, were purchased from New England Biolabs Inc. (Ipswich, MA, USA). The medium LB, used for bacterial growth, was from Merck KgaA (Darmstadt, Germany). Monoclonal M13 antibody labeled with horse-radish peroxide (HRP) was obtained from Abcam Plc. (Cambridge, UK). SEB, bovine serum albumin (BSA), glycerol, Tween 20, polyethylene glycol (PEG), glycine, 2,2′-azino-bis (3-ethylbenziazoline-6-sulfonicacid) (ABTS), *N*-(3-dimethylaminopropyl)-*N*′-ethylcarbodiimide hydrochloride (EDC), N-hydroxy sulfosuccinimide (NHS), 11-mercaptoundecanoic acid (11-MUA), dimethyl sulfoxide (DMSO), and ethanolamine were from Sigma-Aldrich Chemical Co. (St Louis, MO, USA). Na_2HPO_4, KH_2PO_4, Tris, and NaCl, used as PBS and TBS, were from J.T. Baker (Netherlands).

Selection from phage display library

M13 phage display (PhD) library containing 1.5×10^{13} pfu ml^{-1} and 2.7×10^{9} transformants was used to screen against SEB. ELISA plates were coated with the target molecule SEB for screening. The plates were prepared by incubating 150 μg ml^{-1} SEB overnight. After the removal of unbound and weakly bound SEB molecules from the plate, each well was incubated with pH 8.6, 0.1 M carbonate blocking buffer containing 5 mg ml^{-1} BSA. Following the removal of blocking solution, 10 μl of aliquots from PhD library was added on immobilized SEB molecules. After 1 h incubation unbound and weakly bound phages were removed by washing with pH 7.5 TBST buffer (50 mM Tris-HCl, 150 mM NaCl, 0.1% Tween 20). Bound phages were eluted from the SEB surface by using glycine–HCl solution (pH 2.2). To neutralize the well content 1 M Tris–HCl (pH 9.1) was used. Selected phage clones were amplified by infecting liquid *E. coli* culture. The amplified phage clones were separated by centrifugation at (10 000 rpm, 4°C for 10 min). Separated phage clones were purified and concentrated with PEG/NaCl. After incubation the phage clones were pelleted by centrifugation (10 000 rpm, 4°C for 15 min). The phage pellet was dissolved in 0.02% NaN_3 in TBS buffer. Stock solutions of the phage clones were prepared in 50% glycerol.

Phage-ELISA

Selected phage clones were incubated in SEB coated ELISA plates for 1.5 h to determine the affinities of phages to SEB. Unbound and weakly bound phages were removed by washing with TBST (0.5% Tween 20) buffer. HRP-conjugated M13 antibody was brought in contact with phage–SEB complex and then the antibody was incubated for 1.5 h. Following the incubation non-specifically bound antibody conjugates were removed by washing six times with TBST and 200 μl ABST mix solution (21 ml of ABST stock solution was mixed with 36 μl 30% H_2O_2) was added to each well and the enzymatic reaction took place for 30 min. The absorbance at 405 nm was measured by BIO-TEK EL 808 microplate reader (Biotek Instruments, Winooski, VT, USA).

DNA sequencing

Phage particles purification, concentration, and DNA isolation were carried out according to Sambrook *et al*. (1989). Sequencing analysis were done using by Beckmann Coulter CEQ™ 8000 cycle sequencer with −96 sequencing primer (New England BioLab, 5′-GCCCTCATAGTTAGCGTAACG-3′) and 5′-CAGGGATAGCAAGCC CAATA-3′. After DNA sequencing, page displayed peptides were synthesized by solid phase peptide synthesis and purified to 95% purity (GenScript Corp., Piscataway, NJ, USA).

ITC measurements

ITC experiments, carried out to determine the thermodynamic properties of peptide–SEB interactions, were performed at 25°C using a TAM III microcalorimeter (TA Instruments, New Castle, Delaware, USA). The solutions for the experiments were prepared in 50 mM PBS (pH 7.5) except the solutions of peptide4 and SEB used in the titration with peptide4 which included 2% DMSO to increase the solubility of the peptide. All solutions were degassed in an ultrasonic water bath before ITC experiments. Peptide

solutions (0.7 mM) were placed in 250 μl syringe and 800 μl of SEB solution (0.035 mM) was placed in the sample ampoule while the reference ampoule was filled with 800 μl PBS. The peptide solutions were injected into the stirred sample ampoule containing SEB solution in 20 injections (10 μl/injection) by a computer-controlled pump and the heat released with each injection was measured by the calorimeter in dynamic correction mode. Control experiments were performed by titrating peptide solutions into PBS and the heat of binding reaction between the peptides and SEB was obtained as the difference between the heat of reaction and the corresponding heat of dilution. In order to check the specificity of SEB-binding peptides, BSA (0.035 mM) was also titrated by peptide solutions. Binding constants (k), stoichiometry (n), the change in enthalpy (ΔH), the change in free energy (ΔG), and the change in entropy (ΔS) were determined by using the software package of TAM Assistant supplied by TA Instruments.

SPR measurements

Binding of peptide with SEB was investigated by Spreeta™ SPR sensor (Texas Instruments, Dallas, TX, USA) coupled with three-channel flow cell and 12-bit DSP electronic control box. The flow of the reagents was controlled by syringe pumps (Goldman Syringe Pump, Biasis Ltd. Sti., Ankara, Turkey) and four-way switching valves (Upchurch Scientific, Oak Harbor, WA, USA).

Gold coated sensor surfaces were modified with self-assembled monolayer (SAM) of 11-MUA by incubating the surface with 10 mM 11-MUA in absolute ethanol overnight at room temperature. After washing the surface with ethanol and deionized water, the sensors were activated by the solution containing 0.2 M EDC and 0.05 M N-hydroxysulfosuccinimide (NHS) for 1 h. Then activated sensors were incubated with SEB solution (0.014 mM) for 30 min and the surface was blocked with 0.5 M ethanolamine solution. After establishing the baseline with 50 mM PBS (pH 7.5), different concentrations (0.35, 0.70, 1.05, and 1.40 mM) of peptide were injected to the sensor in duplicate for binding to the SEB coated surface.

CD spectroscopy measurements

CD measurements were performed on a JASCO J-810 using a quartz cell of 1.0 mm path length at 25°C. Peptide solutions and SEB solution were prepared in 50 mM, pH 7.5 PBS at a concentration of 50 μM. The concentration of peptides and SEB was 25 μM for CD measurements of peptide–SEB mixture. Spectra were recorded from 195 to 250 nm with a bandwidth of 1.0 nm and a rate of 0.5 nm s^{-1}. Three scans were averaged and corrected for the contribution of buffer solution.

MD simulations

The peptides that showed high affinity to SEB, namely peptide2, peptide3, and peptide5, were constructed using the TINKER molecular modeling package (Ren and Ponder, 2002). The MD simulations initially started from extended (primary) geometries without any bias where the peptides were terminated with N-terminal NH_3^+ and the C-terminal COO^- group. All simulations were performed using The GROMACS molecular modeling package (Van der Spoel *et al*., 2005) in conjunction with OPLS-AA force field (Jorgensen and Severance, 1990). For each simulation, first, peptide system was initially minimized *in vacuo* to remove close van der Waals contacts. This minimization consisted from the steepest descent to conjugate gradient mode. Afterwards, the system was heated at high temperature and then was cooled in constrained simulating annealing *in vacuo* from high temperature to room temperature. After the starting structure chosen from room temperature vacuum conformations, the system was solvated with water molecules in a cubic simulation box. The solvated configuration energy was again minimized from the steepest descent to conjugate gradient methods and so obtained configuration was submitted MD production simulation after thermalization. A similar simulation protocol has been also followed by Drabik *et al*. (2001).

Computational details

The initial energies of our linear peptides were minimized *in vacuo* by using steepest descent and conjugate gradient methods to obtain an energy gradient 100 kJ mol^{-1} nm^{-1}, consecutively. The optimized system was simulated at 1000 K in 100 ps. Afterwards, the system was cooled by simulating annealing from 1000 to 300 K in 200 ps.

The starting structure of each peptide system, obtained from vacuum simulation, was solvated by single point charge water model (SPC) (Berendsen *et al*., 1981). The peptides 2, 3, and 5 contain 2303, 2053, and 2112 water molecules, respectively. Particle Mesh Ewald (PME) summation (Darden *et al*., 1993; Essmann *et al*., 1995) was adopted for long-range electrostatistic interactions with a cut-off 0.9 nm and van der Waals cut-off radius 1.4 nm. The LINCS algorithm (Hess *et al*., 1997) was applied to constrain covalent bonds in the peptides. Periodic boundary conditions were applied and chlorine ion (Cl^-) was added to neutralize the peptide2 for PME methodology. The minimum distance between any atoms of the peptides and simulation box was 1 nm. The starting structures of the peptides with solvent were optimized by energy minimization runs using steepest descent and conjugate gradient algorithms to obtain an energy gradient 100 kJ mol^{-1} nm^{-1}. MD simulation was carried out isobaric, isothermal (NPT) ensemble. Throughout the simulation the solute and solvent were coupled to a constant-temperature ($T = 300$ K) heat-bath and a constant-pressure (1 bar) bath. All simulations were allowed a total thermalization period of 200 ps. The position restrained MD is carried out during this thermalization. Hence, the atomic positions of the peptide were restrained and the water molecules were allowed the equilibrate around the peptides, to remove the solvent holes. In this step, the temperature and pressure were controlled using v-rescale (Bussi *et al*., 2007) and Berendsen baths (Berendsen *et al*., 1984), respectively. Finally, we performed 30 ns MD production simulation using the time step of 2 fs for each peptide. In production runs, the temperature and pressure were controlled using v-rescale and Parrinello–Rahman method (Parrinello and Rahman, 1981) with coupling times 0.1 and 0.5 ps, respectively.

The structures of each peptide in water were characterized by the secondary structure analysis using the definition of proteins (DSSP) protocol (Kabsch and Sander, 1983). The VMD suite software (Humphrey *et al*., 1996) was applied for visualizations.

RESULTS AND DISCUSSION

Phage-ELISA

Peptide phage display library was used to select the SEB binding phages and the affinities of 100 purified phage clones from third

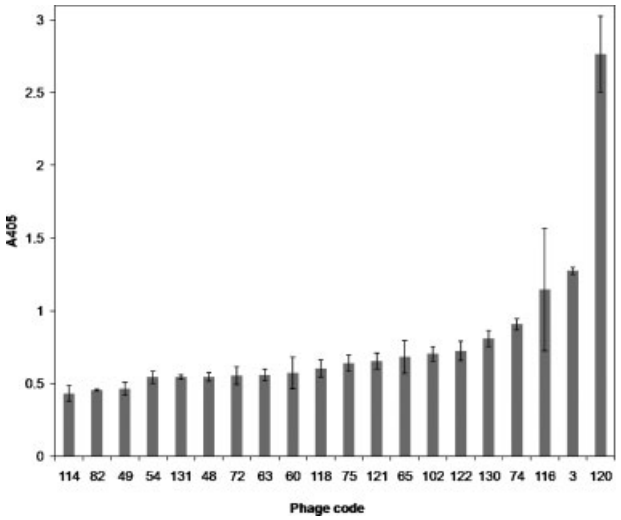

Figure 1. Phage clones that bind to SEB in ELISA. Two hundred microliters of phage clones (10^{10} pfu ml^{-1}) were incubated in SEB coated wells and bound phage clones were detected with HRP conjugated M13 antibody and ABST substrate. Absorbance measurements at 405 nm were done in triplicate and error bars represent the standard deviation.

round of panning were determined by ELISA. Thirteen of the phage clones did not appear to bind SEB. Twenty selected phage isolates elicited high signals when compared with controls (Figure 1). For negative control, phage clones and enzyme-labeled antibodies were incubated in the wells which contain only blocking agent. For positive control, enzyme-labeled antibodies were incubated in SEB coated wells without phage clones.

Sequence analysis

The nucleotide sequences of the random regions of 20 SEB binding phage clones, which elicited high affinities in phage-ELISA, were determined. Of the sequenced phage clones, 16 phage clones revealed the same sequence, although they did not show the same affinity in ELISA. Totally five different sequences were determined as binding to SEB (Table 1). There is not any remarkable sequence similarity between peptides, possibly because they bind to different sites on SEB. All peptides contain at least one positively charged residue, while only three of them have one negatively charged amino acid and selected peptides consist of mostly hydrophilic amino acids.

Table 1. Amino acid sequences of peptides which show high affinity to SEB in phage-ELISA

Peptide code	Amino acid sequence
Peptide1	TQNGMERVTALR
Peptide2	WAPPLFRSSLFY
Peptide3	LLADTTHHRPWT
Peptide4	FTNTSAWLVRYQ
Peptide5	LQGFWQTDASYR

ITC measurements

In order to study the thermodynamic aspects of SEB–peptide interaction, we have used ITC which detected the heat exchanged during the titration of SEB with peptides (Figure 2). The heat of dilution was measured by titrating the peptide into buffer and was subtracted from the measured heat. The single binding site model was used to determine the binding constant (k), stoichiometry (n), and the binding enthalpy (ΔH). Together with the Gibbs free energy (ΔG) and binding entropy (ΔS), the thermodynamic parameters of SEB–peptide interactions are reported in Table 2.

Although the phage clone with peptide1 showed high affinity to SEB in phage-ELISA, the peptide itself did not elicit a binding profile in calorimetric measurement (Figure 2a). Possibly, the synthesized peptide does not have the same affinity to SEB as displayed in the coat protein of phage, since it may have a different geometry when expressed on phage. Similarly, ITC could not produce rewarding results for peptide4 as the baseline noise precluded the measurement of heat of binding, probably due to the low energy of binding and the interference of DMSO used in the buffer to increase the solubility of peptide4 (Figure 2d). The SEB binding peptide2 has an observed binding constant of $1.5 \times 10^4\,M^{-1}$ with a poor binding profile. The binding constant of peptide5 is the same order of magnitude as that of peptide2 with a similar enthalpy value and a better binding transition. In contrast, peptide3 has the highest binding constant value with a very low binding enthalpy. Nevertheless, the enthalpies of binding for all peptides are positive, implying that the complex formation is found to be an endothermic reaction. For the peptides, binding to SEB, the thermodynamics of interaction is dominated by a large positive change in entropy, while the unfavorable enthalpy is a minor component in the free energy of interaction. The main factor giving rise to large favorable entropy is the releasing of ordered water into solution and reduction of water accessible surface during complex formation which emphasizes the importance of hydrophobic residues in SEB–peptide interaction (Jelesarov and Bosshard, 1999).

In parallel, we performed ITC studies on the interaction of SEB binding peptides with BSA in order to check the selectivity of peptides to SEB. Similarly, peptides were titrated into BSA solution to obtain a binding isotherm as well as into buffer alone to obtain heat of dilution (Figure 3). The single binding site model was used to determine the thermodynamic parameters of BSA–peptide interactions (Table 3).

Peptide1 showed a poor binding profile with a binding constant of $1.0 \times 10^4\,M^{-1}$, although it was found to be specific for SEB in the control experiments of phage-ELISA. Similarly, peptide2 bound to BSA with an affinity constant of $7.0 \times 10^3\,M^{-1}$. Interestingly, the interaction of these two peptides with BSA is dominated by favorable enthalpy suggesting a different binding mechanism with the SEB–peptide interaction, probably, due to the importance of different residues on binding. Data evaluation failed for peptide4–BSA interaction as the baseline noise interfered with the binding heat. Peptide3 and peptide5 did not show a binding profile to BSA indicating the selectivity of peptides to SEB.

SPR measurements

In order to investigate the binding of peptide to SEB on a surface, the interaction between SEB and peptide3, which showed the highest affinity to SEB, was studied by SPR sensor. SEB was

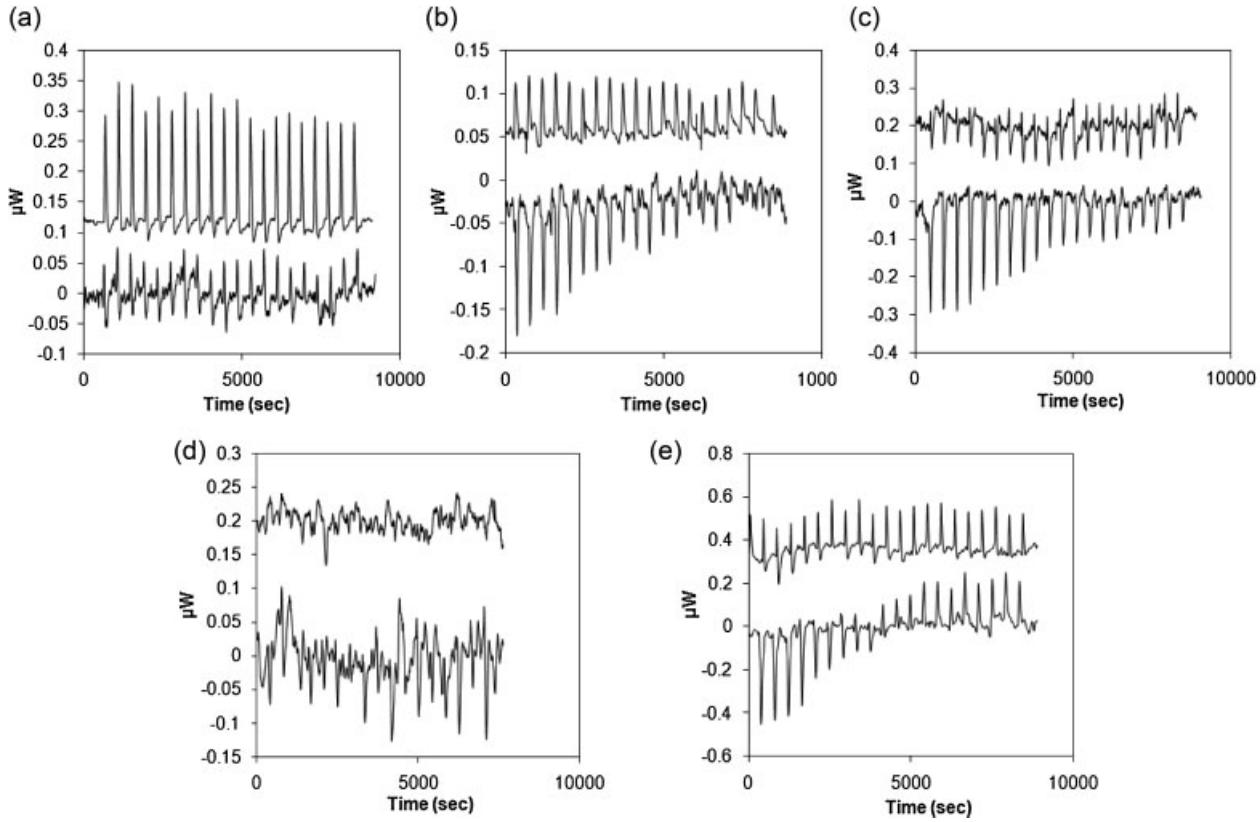

Figure 2. Calorimetric titrations of SEB with (a) peptide1, (b) peptide2, (c) peptide3, (d) peptide4, and (e) peptide5 at 25°C in 50 mM PBS at pH 7.4. The lower curves show the titration of 0.7 mM peptide solutions into the solution of 0.035 mM SEB and the upper curves show the titration of 0.7 mM peptide solutions into buffer.

immobilized on carboxylated thiol modified surface of the SPR sensor. The surface density of SEB was held at a low degree to satisfy the molecular interaction between SEB and peptide3. In order to quantify the interaction between SEB and peptide3, affinity constant of the peptide to SEB coated surface was calculated. Injection of peptide3 solutions at different concentrations yielded the sensorgrams shown in Figure 4, indicating a significant interaction between SEB and peptide. Although ITC binding experiments indicated a 1:1 interaction, the binding data of peptide3 to SEB did not fit to a simple Langmuir interaction model, probably due to the effects of immobilization of SEB to a surface. So, we considered a heterogeneous surface model, including a slower and a faster adsorption site on the surface of the SPR sensor chip. The faster adsorption rate, k_{a1}, is found to be $3.8\,M^{-1}\,s^{-1}$ and for the slower adsorbing region k_{a2} is calculated to be $0.03\,M^{-1}\,s^{-1}$. In contrast, we calculated the desorption rates k_{d1} as $0.014\,s^{-1}$ and k_{d2} as $2 \times 10^{-6}\,s^{-1}$, which reveals that the slower binding region reaches the equilibrium faster than the fast adsorbing sites of SEB on SPR surface. Based on these results, we calculated the affinity constants of the fast and the slow adsorption regions as 2.6×10^2 and $1.6 \times 10^4\,M^{-1}$, respectively. Although the affinity constant of slower region is lower, the affinity constant of faster region is comparable with the affinity constant obtained from the ITC study.

CD spectroscopy measurements

CD experiments were performed to analyze the secondary structure of peptides. CD measurement was not successful for peptide4 due to the effect of DMSO used in the buffer. Far-UV CD

Table 2. Thermodynamic parameters of peptide–SEB interaction derived from ITC

Peptide	K_a (M^{-1})	ΔH (kJ mol^{-1})	ΔG (kJ mol^{-1})	ΔS (J K^{-1} mol^{-1})	n
Peptide1	—	—	—0	—	—
Peptide2	$1.5 \times 10^4 \pm 7.2 \times 10^3$	12.0 ± 1.2	−23.9	120.5	1.01
Peptide3	$2.3 \times 10^5 \pm 4.7 \times 10^4$	5.6 ± 0.4	−30.6	119.8	1.19
Peptide4	—	—	—	—	—
Peptide5	$8.2 \times 10^4 \pm 2.0 \times 10^3$	15.8 ± 0.1	−28.1	147.0	1.01

Binding constant (K_a), enthalpy change (ΔH), Gibbs free energy (ΔG), entropy change (ΔS), and binding stoichiometry (n) are the mean values of two independent titrations.

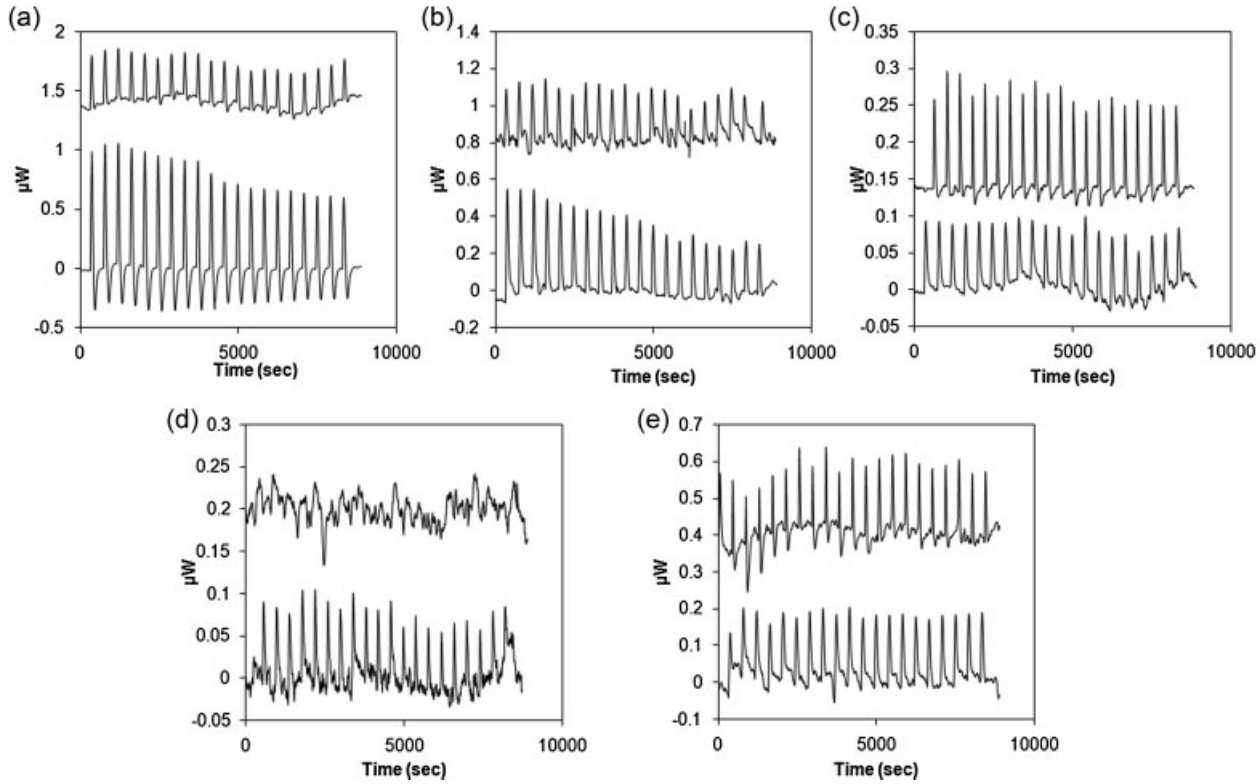

Figure 3. Calorimetric titrations of BSA with (a) peptide1, (b) peptide2, (c) peptide3, (d) peptide4, and (e) peptide5 at 25°C in 50 mM PBS at pH 7.4. The lower curves show the titration of 0.7 mM peptide solutions into the solution of 0.035 mM BSA and the upper curves show the titration of 0.7 mM peptide solutions into buffer.

spectra, recorded for peptides under the same buffer conditions, are shown in Figure 5a. Negative ellipticity band at around 198 nm, found in the spectra of all peptides, indicates random coil structure as expected for such short peptides (Greenfield and Fasman, 1969). Peptide2 shows a positive band at 228 nm, characteristic of poly-proline II helix respecting the two consecutive proline residues in the peptide. The secondary structure contents of peptides, namely α-helix, β-strand, β-turn, and random coil, were calculated by CONTIN program available in the CDPro software package, using the reference set of 37 proteins (Sreerama and Woody, 2000). The estimation of the fraction contents of secondary structures are reported in Table 4. For all peptides, random coil and β-strand structures are dominant, while the proportional content of α-helix is too small. The β-strand content of peptide2 and peptide5 is slightly higher than that of peptide1 and peptide3. The high proportion of β-strand content may be the result of the inadequacy of fitting method for short peptides as the reference set used in the method consists of high molecular weight proteins (Majava *et al*., 2008). Neverthless, the CD spectra of peptides alone show a shape typical of random coil.

In order to analyze the structural effects of complex formation on the SEB binding peptides, the spectra obtained for peptides, incubated with SEB, were compared to that obtained for peptides alone. The difference spectrum obtained by subtracting the SEB spectrum from that of SEB–peptide1 complex is slightly different from the spectrum of peptide1 alone, referring no major conformational change occurred after the incubation. This conformational stability of peptide1 may be due to the low affinity of the peptide to SEB. When compared with the spectra of peptide2, peptide3, and peptide5, the difference spectra of peptides show considerable variations in the intensity and shape

Table 3. Thermodynamic parameters of peptide–BSA interaction derived from ITC

Peptide	K_a (M^{-1})	ΔH (kJ mol^{-1})	ΔG (kJ mol^{-1})	ΔS (J K^{-1} mol^{-1})	n
Peptide1	$1.0 \times 10^4 \pm 7.7 \times 10^3$	-22.0 ± 2.9	-22.8	2.2	0.96
Peptide2	$7.0 \times 10^3 \pm 9.1 \times 10^2$	-22.3 ± 1.8	-22.0	-1.1	0.99
Peptide3	—	—	—	—	—
Peptide4	—	—	—	—	—
Peptide5	—	—	—	—	—

Binding constant (K_a), enthalpy change (ΔH), Gibbs free energy (ΔG), entropy change (ΔS), and binding stoichiometry (n) are the mean values of two independent titrations.

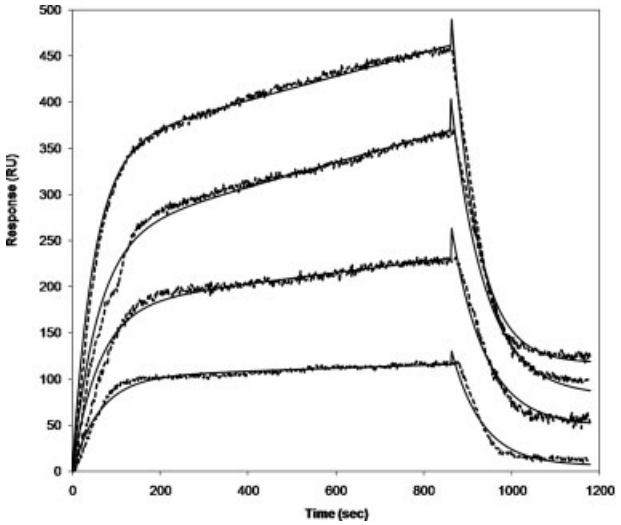

Figure 4. SPR sensorgrams (dashed lines) obtained for the binding of peptide3 in PBS at pH 7.4 to the SEB immobilized surface, fit to the heterogeneous binding model (solid line). All runs are overlaid for peptide concentrations at 0.35, 0.70, 1.05, and 1.40 mM.

Table 4. The average estimation of secondary structure fractions of peptides with the usage of CDPro software package

Peptide	α-Helix	β-Strand	Turn	Random coil	NRMSD[a]
Peptide1	0.07	0.33	0.22	0.38	0.039
Peptide2	0.05	0.38	0.23	0.34	0.046
Peptide3	0.09	0.33	0.22	0.36	0.047
Peptide5	0.05	0.37	0.23	0.35	0.087

[a] Normalized Root Mean Square Deviation.

Table 5. The average estimation of secondary structure fractions of peptides, after interact with SEB, with the usage of CDPro software package

Peptide	α-Helix	β-Strand	Turn	Random coil	NRMSD[a]
Peptide1	0.05	0.35	0.28	0.32	0.218
Peptide2	0.02	0.39	0.53	0.06	0.312
Peptide3	0.02	0.52	0.24	0.22	0.461
Peptide5	0.09	0.44	0.46	0.01	0.275

[a] Normalized Root Mean Square Deviation.

of the ellipticity bands due to the complex formation (Figure 5c). The ellipticity bands centered at 198 nm show positive values indicating the loss of random coil structure. Fitting of the CD spectra using the program CONTIN (Table 5) also indicates a significant decrease in random coil structure and increase in β-strand and β-turn content, suggesting that the peptides gain more ordered structures during the interaction which provide the formation of a stable complex.

MD simulations

While CD gives overall proportions of the main conformational types, it does not specify where in a sequence the particular elements occur. The employing of computational molecular modeling of these peptides from their amino-acid sequences may contribute to understanding their conformational structures. For this reason, MD was performed to the peptides which show high affinity to SEB molecule. Investigation of the time evolution of the secondary structure elements of the peptides for all trajectories is depicted in Figure 6. For all peptides, the first and last residues have random coil structures during the whole simulation. This can be expected due to fact that these terminal residues are in zwitterionic form. For peptide2, it can be seen from Figure 6a, while the initial and final residues (1–2 and 11–12) have random coil structure and around residue 3 the bend structure is dominant, the middle residues are less stable during the simulations. Peptide2 includes two proline residues at positions 3 and 4, which may be the reason for a stable bend structure at this segment as DSSP algorithm does not give an output for the polyproline II helix structure. The middle segments (5–10) have mainly turn and random coil structures as well as a little bit 3-helix during the 3 ns, and then these segments recover the bend and coil structure after 3–7 ns. Although the 3-helix

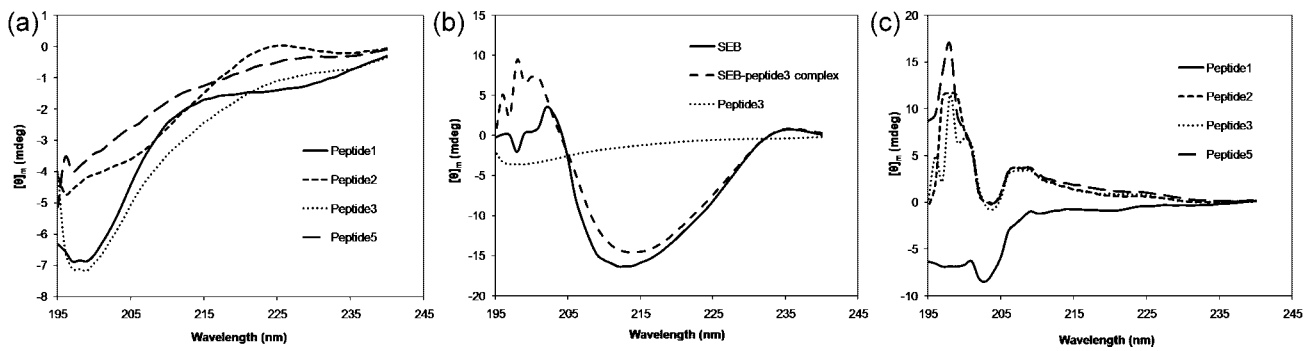

Figure 5. CD spectra of free and bound peptides and SEB. (a) Spectra of free peptides (50 μM) in 50 mM PBS at pH 7.4. (b) Spectra of free peptide3 (25 μM), free SEB (25 μM) and 25 μM SEB incubated with 25 μM peptide3 in 50 mM PBS at pH 7.4. (c) Spectra of bound peptides obtained by subtracting the SEB spectrum from that of SEB–peptide complex.

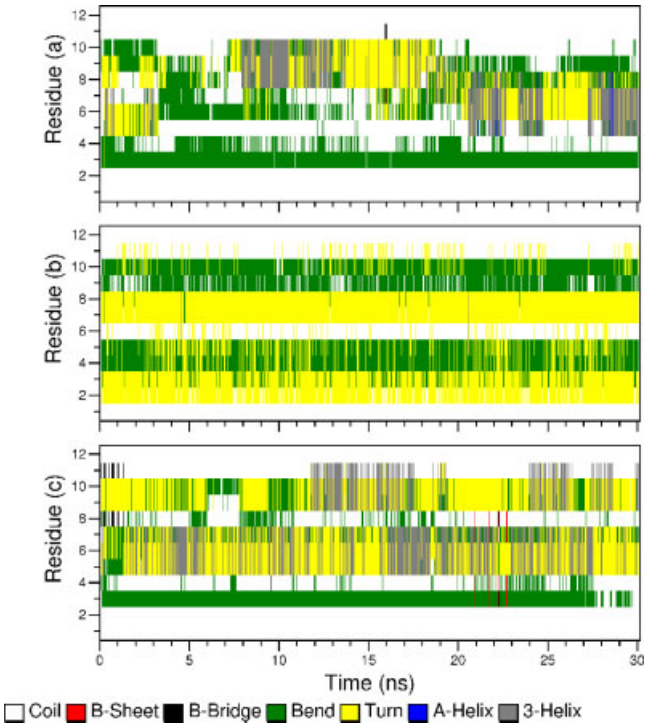

Figure 6. Secondary structure assignment per residue of (a) peptide2, (b) peptide3, and (c) peptide5 plotted versus time for all trajectories.

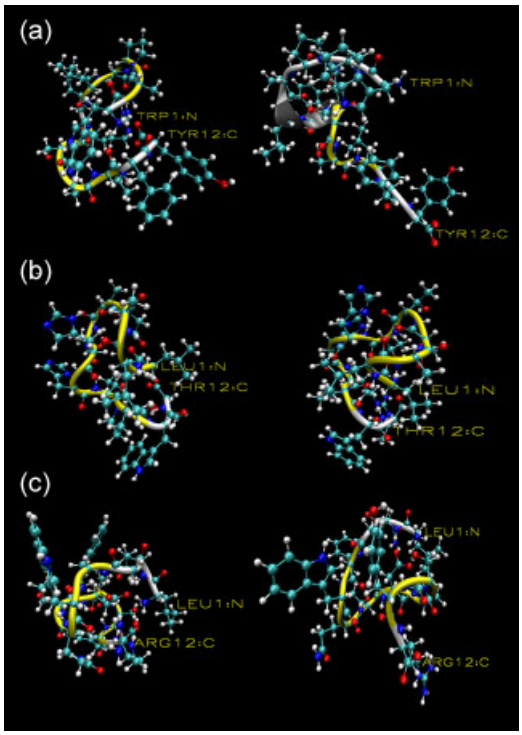

Figure 7. Representative structures of (a) peptide2, (b) peptide3, and (c) peptide5 for initial (left) and final (right) structures obtained during 30 ns simulations. The residues involved in the turn, random coil, and 3-helix are shown by yellow, white, and gray newcartoon, respectively. Atoms are colored red for oxygen, blue for nitrogen, white for hydrogen, and cyan for carbon.

structure mostly appears, especially at residues 8–10 between 7 and 14 ns, these residues adopt turn between 14 and 19 ns as the serine residues, at positions 8 and 9, prefer to be in turn structure. On the other hand, after 19 ns, while residues 9–10 have bend and coil structures, residues 5–8 have turn and 3-helix structure with a little bit α-helix at the rest of simulation. In Figure 6b, for peptide3, during the whole simulation, the residues 1, 6, and 11–12 adopt completely random coil structure. On the other hand, while the segments 2–3, having leucine and alanine residues, and 7–8, having two histidine residues, adopt turn structures, segments 9–10 have mainly bend structure. For the segments 4–5, the bend structures appeared at the beginning of simulations, these are destroyed and a mixture of turn and bend structures are formed at the rest of the simulation. For peptide5, residues 1–2, 4, and 11–12 mainly adopt random coil structure. The residue 3 has bend structure during the whole simulation. The residues 5–7 and 9–10 have a mixture of turn, 3-helix, and bend structures, but, it can be seen from the Figure 6c, the portions of turn structures is more than 3-helix and bend ones. Although the residues 8 and 11 have β-bridge structure (single pair β-sheet hydrogen bond formation) at the beginning of the simulation, their structure is rapidly replaced with the coil, bend, coil and 3-helix structures after 1.5 ns, respectively. On the other hand, after 21 ns, some conformations show β-sheet structures at the residues 3–4 and 7–8, and β-bridge at residue 3 and 8. Although CD spectroscopy measurements reveal that these peptides exist mainly as random coil, β-sheet, and turn conformations in aqueous solution, no β-sheet structure is observed for peptide2 and peptide3 sequences. For visualizations, the initial structures of each peptide and the snapshots of their final structures in water are also shown in Figure 7.

CONCLUSIONS

Phage display selected SEB binding peptides were analyzed for their binding affinity using ITC and SPR. These binding affinity studies were coupled with secondary structure studies. First ITC was employed to understand the binding energetic of the peptide ligands for their binding to SEB molecule. Among the peptides tested, peptide3 was found to have the highest affinity for SEB, also peptide2 and peptide5 seemed to have strong interaction with the SEB molecules. But the other peptides, peptide1 and peptide4, did not show a significant heat signature during the ITC experiments. Since all of these peptides screened on phages were selected as the best binders from ELISA experiments, it is clear that the peptide in a framework such as the coat protein of the phage body may not have the same binding activity as its free peptide form. Not only the binding affinity, but also the selectivity of the peptide ligands for their target molecules is crucial for their utilization in actual applications. The cross specificity of the SEB binding peptide ligands toward a commonly used protein, BSA, was tested. Peptide1 and peptide2 showed some degree of affinity toward BSA. The affinity of peptides1 was significant compared to its non-binding to SEB. On the other hand the other two peptides, peptide3 and peptide5, do not show a significant heat signature for their interaction with BSA molecule. SPR experiments with the best binder, peptide3, reveals a two stage binding. Due to the immobilization of SEB on SPR chip surface, sites of SEB exposed to the interaction with peptide ligand may not be homogenous.

This makes the available sites of SEB limited, so the peptide interacts faster and desorbs faster at some of the sites, as it was adsorbed slowly and desorbs slowly at different binding sites. However, the desorption of the peptide3 at the slow interacting sites of SEB is remarkably slow, compared to the fast adsorption sites. This is may be due to the structural rearrangement of the peptide at these sites, which directs a tighter binding of the peptide on SEB molecule.

Besides the affinity studies, structural properties of the peptide ligands are playing a crucial role for the molecular recognition. As stated earlier the peptides are expected to have a random secondary structure in solution, which may increase their capability to interact with the target protein easily. The high content of the random coil type secondary structure in the peptides is expected as these peptides cannot fold into more structured orientations because of their short amino acid chains. Not surprisingly all of the peptides have the same secondary structure elements at almost same ratios. So this result does not support any correlation between the binding activity of the peptides and structural properties of the peptides. There is barely a difference between a good binder peptide3 and non-binding peptide, peptide 1, by means of the ratio of the secondary structure elements. However, after the interaction of the peptides with the SEB molecule, there is a remarkable decrease in the random coil content of the peptides which is a signature for the formation of the more ordered assembly of the peptide ligand on the surface of SEB molecule. However, the decrease in the random coil content is not same for all of the peptide ligands. The random coil content of peptide2 and peptide5 decreased dramatically, but the decrease in the random coil content of the peptide3 is less remarkable compared to the other peptides. Secondary structure rigidity of peptide1, with only a slight decrease in the random coil content, may be responsible for the non-binding of this peptide. Another significant increase is in the turn content of the peptide2 and peptide5, which is not the case for the peptide3. The change in the sheet content during the interaction with SEB is only remarkable for peptide3. For the SEB binding peptides, it seems that peptide2 and peptide5 have the similar binding pattern, however, the peptide3 does not resemble to these peptides. This may be the reason for the better binding of the peptide3 compared to the peptide2 and peptide5. This peptide does not have a significant increase in the turn content and the sheet structure seems to be more favorable for a tighter binding to SEB molecule.

The results of the MD simulations support the outcomes of CD as the peptides show mainly unordered structures. MD results state that while the residues in the N- and C-terminal of the peptides show mainly random coil structure, the middle parts are dominated by turns and bends. Those turns may be responsible for the specific binding of peptides to SEB and the random coil structures at the two terminals may provide flexibility to peptides which increases the affinity.

Our results demonstrate the importance of hydrophobic residues for affinity of SEB binding peptide ligands. In addition, the unstable structures of peptides, before binding to SEB, negatively impacts binding, which may provide evidence to support the importance of secondary structures of aptamers on binding affinity, even in such short peptides. Furthermore, interaction of peptide3 to SEB can be fine-tuned by modifications at contact residues that contribute energetically to the binding, while keeping the structural epitopes stable. In the light of our findings, a more detailed analysis is needed to determine the core amino acids which are responsible for the binding of the peptides to SEB. To carry out this, point mutations by changing positions of amino acids and replacing certain amino acids will be carried out which we suppose will lead us to engineer superior binding peptides with high selectivity.

The structure–activity relationship is the key for the understanding of the molecular recognition mechanism of the peptide ligands. To design more robust peptide aptamers, one can use the clues from the affinity and structure experiments and can tune the mode of binding for tighter binding of the peptides. The control of the structure of the available immunologic agents needs complex tools, which makes it hard to tune their binding capabilities on a biosensor surface. However, peptide aptamers promise a more robust and controlled detection of their target agents as a good candidate of molecular recognition elements of a biosensor through supramolecular interactions.

Acknowledgements

The authors wish to thank Professor Aykut Özkul (Ankara University, Turkey) for analyzing DNA sequences. This study has been financially supported by The Scientific and Technological Research Council of Turkey (TUBITAK) with the project number 108O031.

REFERENCES

Berendsen HJC, Postma JPM, van Gunsteren WF, Dinola A, Haak JR. 1984. Molecular dynamics with coupling to an external bath. *J. Chem. Phys.* **81**: 3684–3690.

Berendsen HJC, Postma JPM, van Gusteren WF, Hermans J. 1981. Interaction Models for Water in Relation to Protein Hydration. D. Reidel: Dordrecht; 331–342.

Bussi G, Donadio D, Parrinello M. 2007. Canonical sampling through velocity rescaling. *J. Chem. Phys.* **126**: 014101.

Darden T, York D, Pedersen L. 1993. Particle mesh Ewald: an N.log(N) method for Ewald sums in large systems. *J. Chem. Phys.* **98**: 10089–10092.

Drabik P, Liwo A, Czaplewski C, Ciarkowski J. 2001. The investigation of the effects of counterions in protein dynamics simulations. *Protein Eng. Des. Sel.* **14**: 747–752.

Enever C, Tomlinson IM, Lund J, Levens M, Holliger P. 2005. Engineering high affinity superantigens by phage display. *J. Mol. Biol.* **347**: 107–120.

Essmann U, Perera L, Berkowitz ML, Darden T, Lee H, Pedersen LG. 1995. A smooth particle mesh Ewald method. *J. Chem. Phys.* **103**: 8577–8593.

Goldman ER, Pazirandeh MP, Mauro JM, King KD, Frey JC, Anderson GP. 2000. Phage-displayed peptides as biosensor reagents. *J. Mol. Recognit.* **13**: 382–387.

Goud H, Yanai Y, Sugawar A, Sunazuka T, Omura S, Hirono S. 2008. Computational analysis of the binding affinities of the natural-product cyclopentapeptides argifin and argadin to chininase B from Serratia marcescens. *Bioorg. Med. Chem.* **16**: 3565–3579.

Greenfield N, Fasman GD. 1969. Computed circular dichroism spectra for the evaluation of protein conformation. *Biochemistry* **8**: 4108–4116.

Harteveld JLN, Nieuwenhuizen MS, Wils ERJ. 1997. Detection of staphylococcal enterotoxin B employing a piezoelectric crystal immunosensor. *J. Microbiol. Meth.* **7**: 661–667.

Hess B, Bekker H, Berendsen HJC, Fraaije JGEM. 1997. LINCS: a linear constraint solver for molecular simulations. *J. Comput. Chem.* **18**: 1463–1472.

Homola J, Dostalek J, Chen S, Rasooly A, Jiang S, Yee SS. 2002. Spectral surface plasmon resonance biosensor for detection of staphylococcal enterotoxin B in milk. *Int. J. Food Microbiol.* **7**: 61–69.

Humphrey W, Dalke A, Schulten K. 1996. VMD: Visual molecular dynamics. *J. Mol. Graph.* **14**: 33–38.

Jelesarov I, Bosshard HR. 1999. Isothermal titration calorimetry and differential scanning calorimetry as complementary tools to investigate the energetic of biomolecular recognition. *J. Mol. Recognit.* **12**: 3–18.

Jorgensen WL, Severance DL. 1990. Aromatic-aromatic interactions: free energy profiles for the benzene dimer in water, chloroform, and liquid benzene. *J. Am. Chem. Soc.* **112**: 4768–4774.

Kabsch W, Sander C. 1983. Dictionary of protein secondary structure: pattern recognition of hydrogen bonded and geometrical features. *Biopolymers* **22**: 2577–2637.

King KD, Anderson GP, Bullock KE, Regina MJ, Saaski EW, Ligler FS. 1999. Detecting staphylococcal enterotoxin B using an automated fiber optic biosensor. *Biosens. Bioelectron.* **14**: 163–170.

Klepeis JL, Lindorff-Larsen K, Dror RO, Shaw DE. 2009. Long-timescale molecular dynamics simulations of protein structure and function. *Curr. Opin. Struc. Biol.* **19**: 120–127.

Ladner RC, Sato AK, Gorzelany J, Souza M. 2004. Phage display-derived peptides as therapeutic alternatives to antibodies. *Drug Discov. Today* **9**: 525–529.

Ler SG, Lee FK, Gopalakrishnakone P. 2006. Trends in detection of warfare agents: detection methods for ricin, staphylococcal enterotoxin B and T-2 toxin. *J. Chromatogr. A* **1133**: 1–12.

Lin HC, Tsai WC. 2003. Piezoelectric crystal immunosensor for the detection of staphylococcal enterotoxin B. *Biosens. Bioelectron.* **18**: 1479–1483.

Majava V, Petoukhov MV, Hayashi N, Pirila P, Svergun DI, Kursula P. 2008. Interaction between the C-terminal region of human myelin basic protein and calmodulin: analysis of complex formation and solution structure. *BMC Struct. Biol.* **8**: 10.

Mourez M, Kane RS, Mogridge J, Metallo S, Deschateletes P, Sellman BR, Whitesides GM, Collier RJ. 2001. Designing a polyvalent inhibitor of anthrax toxin. *Nat. Biotechnol.* **19**: 958–961.

Naimushin AN, Soelberg SD, Nguyen DK, Dunlap L, Bartholomew D, Elkind J, Melendez J, Furlong CE. 2002. Detection of *Staphylococcus aureus* enterotoxin B at femtomolar levels with a miniature integrated two-channel surface plasmon resonance (SPR) sensor. *Biosens. Bioelectron.* **17**: 573–584.

Parrinello M, Rahman A. 1981. Polymorphic transitions in single-crystals: a new molecular dynamics method. *J. Appl. Phys.* **52**: 7182–7190.

Petrenko VA, Vodyanoy VJ. 2003. Phage display for detection of biological threat agents. *J. Microbiol. Meth.* **53**: 253–262.

Petrenko VA, Sorokulova IB. 2004. Detection of biological threats: a challenge for directed molecular evolution. *J. Microbiol. Meth.* **58**: 147–168.

Ren PY, Ponder JW. 2002. Consistent treatment of inter- and intramolecular polarization in molecular mechanics calculations. *J. Comput. Chem.* **23**: 1497–1506.

Sambrook J, Fritsch EF, Maniatis T. 1989. Molecular Cloning-A Laboratory Manual, 2nd edn. Cold Spring Harbor Laboratory Press: New York.

Samoylov AM, Samoylova TI, Pathirana ST, Globa LP, Vodyanoy VJ. 2002. Peptide biosensor for recognition of cross-species cell surface markers. *J. Mol. Recognit.* **15**: 197–203.

Sarikaya M, Tamerler C, Jen AKY, Schulten K, Baneyx F. 2003. Molecular biomimetics: nanotechnology through biology. *Nat. Mater.* **2**: 577–585.

Schaeffer RD, Fersht A, Daggett V. 2008. Combining experiment and simulation in protein folding: closing the gap for small model systems. *Curr. Opin. Struct. Biol.* **18**: 4–9.

Seibert M, Patrickson A, Hess B, van der Spoel D. 2005. Reproducible polypeptide folding and structure prediction using molecular dynamic simulations. *J. Mol. Biol.* **354**: 173–183.

Sidhu SS, Fairbrother WJ, Deshayes K. 2003. Exploring protein-protein interactions with phage display. *Chem. Bio. Chem.* **4**: 14–15.

Slavik R, Homola J, Brynda E. 2002. A miniature fiber optic surface plasmon resonance sensor for fast detection of staphylococcal enterotoxin B. *Biosens. Bioelectron.* **17**: 591–595.

Smith GP. 1985. Filamentous fusion phage: novel expression vectors that display cloned antigens on the virion surface. *Science* **228**: 1315–1317.

Smith GP, Petrenko VA. 1997. Phage display. *Chem. Rev.* **97**: 391–410.

Soykut EA, Dudak FC, Boyacı İH. 2008. Selection of staphylococcal enterotoxin B (SEB)-binding peptide using phage display technology. *Biochem. Bioph. Res. Co.* **370**: 104–108.

Sreerama N, Woody RW. 2000. Estimation of protein secondary structure from circular dichroism spectra: comparison of CONTIN, SELCON, and CDSSTR methods with an expanded reference set. *Anal. Biochem.* **287**: 252–260.

Turnbough CL Jr. 2003. Discovery of phage display peptide ligands for species-specific detection of *Bacillus* spores. *J. Microbiol. Meth.* **53**: 263–271.

Van der Spoel D, Lindahl E, Hess B, Groenhof G, Mark AE, Berendsen HJC. 2005. GROMACS: Fast, flexible, and free. *J. Comput. Chem.* **26**: 1701–1718.

Wang G, De J, Schoeniger JS, Roe DC, Carbonell RG. 2004. A hexamer peptide ligand that binds selectively to staphylococcal enterotoxin B: isolation from a solid phase combinatorial library. *J. Peptide Res.* **64**: 51–64.

Zdanovsky AG, Karassina NV, Simpson D, Zdanovskaia MV. 2001. Peptide phage display library as source for inhibitors of clostridial neurotoxins. *J. Protein Chem.* **20**: 73–80.

Zhao SW, Shen PP, Zhou Y, Wei Y, Xin XB, Hua ZC. 2005. Selecting peptide ligands of microcystin-LR from phage displayed random libraries. *Environ. Int.* **31**: 535–541.